Temperature and pH Dependence of the Metarhodopsin I–Metarhodopsin II Kinetics and Equilibria in Bovine Rod Disk Membrane Suspensions†

John H. Parkes and Paul A. Liebman*

ABSTRACT: The kinetics of the relaxation of bleached bovine rod disk membrane suspensions from metarhodopsin I into the equilibrium between metarhodopsins I and II were determined at pHs between 5.9 and 8.1 and at temperatures between −1 and 15 °C. From these data, thermodynamic equations were generated by two-way linear regression that simultaneously describe the functional dependence on pH and temperature of the pseudo-first-order and true forward rate constants, the reverse and observed rate constants, and the equilibrium constant. Using these equations, we obtained the thermodynamic parameters and the apparent net proton uptake for the transitions from metarhodopsin I to metarhodopsin II and from metarhodopsin I to the activated intermediate. The reversibility of this equilibrium and the effect of aging of the preparation on the measured rate constants were investigated.

Rhodopsin, upon illumination by a brief light flash, bleaches spontaneously through a series of spectral intermediates, including metarhodopsins I and II (MI and MII),[1] before separating into *all-trans*-retinal and opsin (Matthews et al., 1963; Ostroy et al., 1966). MII is probably the first of these intermediates that can catalyze the binding of GTP to G protein (Γ) (Parkes et al., 1979; Somers & Shichi, 1982) which then activates retinal phosphodiesterase (PDE). PDE in turn hydrolyzes cGMP, and this reaction may modulate the diffusible messenger that transmits the light-reception signal to the plasma membrane (Liebman & Pugh, 1979, 1981; Mueller & Pugh, 1983; Liebman et al., 1983.) The formation of MII is rate limiting in the activation of the hydrolysis of cGMP, while the fraction of bleached rhodopsin converted to MII affects the overall gain of the system, that is, the number of molecules of cGMP hydrolyzed per photon absorbed. An accurate understanding of this equilibrium is thus of particular importance in the study of visual excitation.

The MI–MII equilibrium has been the subject of a number of studies since the original work by Matthews et al. (1963), but the existing literature on the kinetics of this reaction has been largely confined to studies of the observed rate constant (k_{obs}). Baumann and co-workers (Baumann & Reinheimer, 1973; Baumann, 1978; Baumann & Zeppenfeld, 1981) have determined the equilibrium and forward rate constants for the MI–MII equilibrium in the frog and from this have calculated the thermodynamic parameters for the MI → MII reaction and the activation of MI, but even their work was limited to the temperature dependence at one pH and the pH dependence at one temperature. The equilibrium pK and temperature dependence for the frog MI–MII reaction are very different from those of cattle, and an analysis such as that of Baumann has not been done for any homeothermic animal species. A general formulation including both pH and temperature has not been undertaken heretofore on any species.

Thus, in analyzing the individual steps in the overall kinetics of PDE activation, we could neither find nor calculate from the literature rate or equilibrium constants for the MI–MII reaction at the pHs and temperatures we employed. In generating this experimental information, we also found it of interest to calculate the thermodynamic parameters of the overall reaction, MI → MII, and to compare these with the parameters of the activation reaction, MI → M$^+$. [Earlier work (Ebrey, 1978; Lewis et al., 1981) using k_{obs} as an approximation for the forward rate constant is at best only approximately correct.] Since a systematic study of pH dependence was done, it was possible to determine whether the reaction is both acid and base catalyzed, as previously reported (Emrich & Reich, 1974), or whether the apparent acid catalysis is only a mass-action effect of the proton taken up in the reaction. In answering these questions, we devised general equations for the MI–MII equilibrium and the individual rate constants as a function of pH and temperature, and from these, we determined the thermodynamic quantities for the formation of MII from MI and for the activation of MI to M*. The following section briefly reviews the theory of the equilibrium kinetics to show how the rate constants may be determined.

Mathematical Analysis

The equilibrium reaction between MI and MII involves some hydrogen ion uptake (Radding & Wald, 1956; Falk & Fatt, 1966; Wong & Ostroy, 1973; Bennett, 1978):

$$\mathrm{MI} + n\mathrm{H}^+ \underset{k_{-1}}{\overset{k'_1}{\rightleftharpoons}} \mathrm{MII} \qquad (1)$$

Thus, while the back-reaction is unimolecular, having an experimental first-order rate constant, k_{-1}, the forward reaction has a higher intrinsic molecularity, and its experimental rate constant, k'_1, will be greater than first order unless the proton concentration remains constant. If it is assumed that the internal buffering maintains an essentially constant [H$^+$], the reaction can be written as a pseudo-first-order one:

$$\mathrm{MI} \underset{k_{-1}}{\overset{k_1}{\rightleftharpoons}} \mathrm{MII} \qquad (2)$$

where $k_1 = [\mathrm{H}^+]^n k'_1$.

† From the Departments of Anatomy and Ophthalmology, School of Medicine, University of Pennsylvania, Philadelphia, Pennsylvania 19104. *Received January 11, 1984.* This work was supported by U.S. Public Health Service Grants EY00012 and EY01583 and by a Biomedical Research Support Grant from the University of Pennsylvania.

* Address correspondence to this author at the Department of Anatomy, School of Medicine, University of Pennsylvania.

[1] Abbreviations: cGMP, guanosine cyclic 3′,5′-phosphate; Γ, G protein; k_{obs}, observed rate constant; MI, metarhodopsin I; MII, metarhodopsin II; MIII, metarhodopsin III; M*, activated intermediate in the MI–MII equilibrium; n^*, coefficient of apparent proton uptake in the reaction MI → M*; PDE, retinal phosphodiesterase; RDM, rod disk membrane(s); Rh, rhodopsin; MOPS, 3-(*N*-morpholino)propanesulfonic acid; EDTA, ethylenediaminetetraacetic acid; DTT, dithiothreitol.

0006-2960/84/0423-5054$01.50/0

If it is assumed that no significant amount of metarhodopsin III (MIII) or free retinal plus opsin is formed during the establishment of the equilibrium between MI and MII, then essentially all of the bleached rhodopsin is converted either to MI or to MII. Thus, one can write

$$[\mathrm{Rh}] = [\mathrm{MI}] + [\mathrm{MII}] \tag{3}$$

In this and the equations that follow, [Rh] is the amount of rhodopsin bleached by a single flash, and [MI] and [MII] are the amounts of the metarhodopsins formed by that bleach. To simplify the notation, any dependence on wavelength or time has been omitted.

A related conservation equation states that, immediately subsequent to the conversion of bleached rhodopsin to MI, the only reaction of significance is the interconversion between MI and MII, i.e.

$$\frac{\mathrm{d[MI]}}{\mathrm{d}t} = -\frac{\mathrm{d[MII]}}{\mathrm{d}t} \tag{4}$$

Note that once the equilibrium between MI and MII has been established, the RDM suspension will respond to a subsequent bleach as if there were no MI or MII already formed. The gradual production of MIII or retinal and opsin does not invalidate these relationships for successive bleaches, since their rates of formation are so slow that MI and MII remain in equilibrium. Thus, except for the problem of enhanced MII formation, discussed below, the time course of MII formation on successive bleaches should be the same, and the data can be averaged.

Following the initial formation of MI, the rate of change in the absorbance at a particular wavelength can be written

$$\frac{\mathrm{d}A}{\mathrm{d}t} = e_{\mathrm{MI}}\frac{\mathrm{d[MI]}}{\mathrm{d}t} + e_{\mathrm{MII}}\frac{\mathrm{d[MII]}}{\mathrm{d}t} \tag{5}$$

where the absorbance is measured from the moment after the flash when the bleached rhodopsin is fully converted to MI but little MII has yet formed. Using conservation eq 4, and defining Δe as the difference between the extinction coefficients for MII and MI ($e_{\mathrm{MII}} - e_{\mathrm{MI}}$), we have

$$\frac{\mathrm{d}A}{\mathrm{d}t} = \Delta e\frac{\mathrm{d[MII]}}{\mathrm{d}t} \tag{6}$$

The net rate of formation of MII obtained from eq 2 is

$$\frac{\mathrm{d}A}{\mathrm{d}t} = \Delta e(k_1[\mathrm{MI}] - k_{-1}[\mathrm{MII}]) \tag{7}$$

Using conservation eq 3, we can write this as

$$\frac{\mathrm{d}A}{\mathrm{d}t} = \Delta e\{k_1[\mathrm{Rh}] - (k_1 + k_{-1})[\mathrm{MII}]\} \tag{8}$$

Defining $k_{\mathrm{obs}} = k_1 + k_{-1}$, we have

$$\frac{\mathrm{d}A}{\mathrm{d}t} = \Delta e(k_1[\mathrm{Rh}] - k_{\mathrm{obs}}[\mathrm{MII}]) \tag{9}$$

The justification for referring to an "observed" rate constant is seen more clearly in the integral form of eq 9:

$$\Delta A = \Delta e[\mathrm{MII}] = \frac{k_1}{k_{\mathrm{obs}}}\Delta e[\mathrm{Rh}](1 - e^{-k_{\mathrm{obs}}t}) \tag{10}$$

which relaxes to its final value with the rate constant k_{obs}. Evaluating eq 9 at $t = 0$, we find

$$k_1 = \frac{[(\mathrm{d}/\mathrm{d}t)A]_{t=0}}{\Delta e[\mathrm{Rh}]} \tag{11}$$

Either eq 9 or eq 10 can be evaluated at t = infinity to give the fraction of bleached rhodopsin converted to MII:

$$[\mathrm{MII}]/[\mathrm{Rh}] = k_1/k_{\mathrm{obs}} \tag{12}$$

To calculate k_1, one need only measure k_{obs} and [Rh] and determine the initial rate of change of the optical density. From these, Δe, and the pH of the sample, k'_1, k_{-1}, and [MII]/[Rh] can be calculated.

It might appear that if the fraction of rhodopsin converted to MII were known, eq 12 could be used to determine k_1 independently of any estimate for Δe. But to know, from the ΔA of the reaction at a given temperature and pH, how much MII was formed requires knowing how large the ΔA would be if all the rhodopsin bleached by one flash were converted to MII, and this is equivalent to knowing Δe. On the basis of our own experiments and from published data in the literature (Rafferty, 1979), we used the value of 33 000 L/(mol·cm) for the value of Δe at 390 nm. This probably represents a lower limit on the actual value, as it is difficult to determine that the reaction has gone quantitatively to MII.

Materials and Methods

Rod disk membrane (RDM) suspensions consisting largely of isolated disks were prepared by using a standard sucrose floatation method described previously (Yee & Liebman, 1978) under infrared or dim red light from frozen bovine retinas (Hormel) in a medium of 20 mM MOPS (pK = 7.20 at 20 °C), 100 mM KCl, 2 mM $MgCl_2$, 100 μM EDTA, and 1 mM DTT. Suspensions were typically 12–14 μM in rhodopsin. The pHs were adjusted on separate aliquots of each preparation and allowed to equilibrate, usually overnight. Initial concentrations were determined from the absorption at 600, 500, and 400 nm, by using the Dartnall correction for scattering[2] (Knowles & Dartnall, 1977). Samples were cooled to the desired temperature in the thermally jacketed cuvette holder of an Aminco DW-2 spectrophotometer. The preparations were partially bleached by a series of flashes from a xenon flashlamp at 50-s intervals, each flash bleaching about 10% of the remaining visual pigment. A prebleach base line and the postbleach kinetics were recorded at 390 nm, with a 650-nm reference (dual beam), and the data were stored and analyzed by using a PDP 11-03 computer.

To demonstrate the reversibility of the MI–MII equilibrium, identical suspensions of RDM were placed in the sample and reference cuvettes of the spectrophotometer and cooled to 2 °C. To eliminate any differential effects due to scattering or enhanced MII formation present at small bleaches, both cuvettes were bleached with four flashes from the xenon flashlamp. The location of the flash was such that about 50% of the rhodopsin in the sample cuvette was bleached, while only about 20% of the rhodopsin in the reference cuvette was bleached. A difference spectrum between the 50% and 20% bleached samples was recorded, equal aliquots of NaOH or HCl were added to each, and the difference spectrum was again recorded. In this fashion, the RDM suspensions were cycled several times between more acidic and more basic pHs. Finally, the differences between consecutive difference spectra were obtained, showing the change in absorbance produced by each change in pH attributable to the greater amount of bleached rhodopsin in the sample cuvette. The successive difference spectra upon addition of H^+ and OH^- were found after correction for dilution to be the exact inverse of the proceeding and succeeding spectrum, showing that MI and

[2] $[\mathrm{Rh}] = (1.1\mathrm{OD}_{500} - 0.77\mathrm{OD}_{600} - 0.33\mathrm{OD}_{400})/40\,000$.

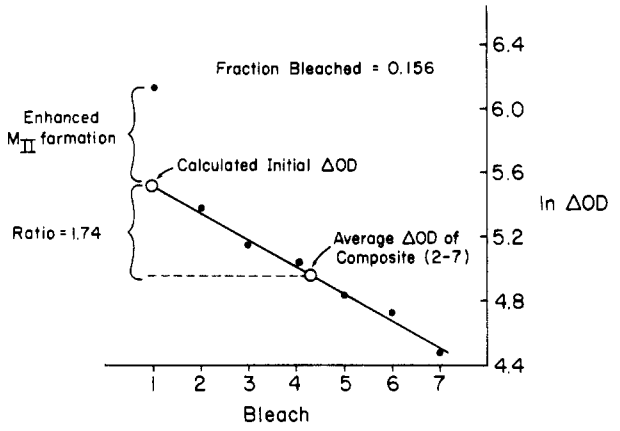

FIGURE 1: Method of data analysis. The kinetic response curve of an RDM preparation to a bleaching flash was fit to a single first-order exponential equation. The rate constant of this equation is k_{obs} and k_1 can be determined from the initial slope and the rhodopsin concentration of the composite average. The ΔOD's observed on successive bleaches are plotted on a semilog scale. From this, the fraction bleached, the concentration ratio, and the degree of MII enhancement can be determined.

MII are in fact pairs of a rapidly reversible equilibrium.

We also compared the absorption spectrum measured after the initial bleaches with that obtained after consecutive additions of HCl and NaOH. In the former case, the equilibrium was reached from a condition of excess MI; in the latter case, it would have been reached from a condition of excess MII. Within the accuracy of the measurements, the spectra were identical.

Data Analysis

The data obtained following each bleaching flash were fit to a single exponential, which was then extrapolated back to the time of the flash to determine the initial slope. Because the high voltage to the photomultiplier tube of the spectrophotometer was controlled through a feedback loop, meaningful data could not be obtained for about 60 ms after the flash, even if the photomultiplier was protected from the flash by using crossed optical filters. This imposed an upper limit to the temperature at which the reaction could be studied by using this apparatus, since at temperatures above 15 °C, the reaction proceeded too nearly to completion within the first 60 ms to permit accurate analysis.

The increase in optical density after each flash was plotted on a logarithmic scale, and the fraction of rhodopsin bleached by each flash was determined from the slope of the regression line fit to these data points (Figure 1). The linearity of these points on the logarithmic decrement curve provides evidence supporting the assumption that little MIII was formed during the time course of the experiment and that the efficiency of bleaching was not changing due to the formation of isorhodopsin.

It was noted, however, that if the RDM suspension had been prepared under infrared light, the first bleaching flash produced an abnormally large, slow change in optical density (Figure 1). It is now understood that this was due to stabilization of MII by G protein (Γ) (Emeis & Hofmann, 1981; Bennett et al., 1982). The sequence of reactions involving MII and Γ is believed to proceed as follows:

$$MI \rightleftharpoons MII \xrightarrow{\Gamma\cdot GDP} MII\cdot\Gamma\cdot GDP \xrightarrow{GTP\ \ GDP} MII + \Gamma\cdot GTP$$

MII is apparently stabilized by binding to Γ, so that, in the absence of GTP, an excess amount of MII (actually MII·Γ·GDP) was formed at low bleaches. Further stabilization ceased, however, once all the Γ was used up, which occurred when about 10% of the rhodopsin was bleached.

In the presence of 250 μM GTP or more, enhanced MII formation does not occur, since GTP exchanges with GDP in the MII·Γ complex, immediately releasing the MII (J. H. Parkes and P. A. Liebman, unpublished experiments). Enhanced formation of MII is thus an artifact of the RDM preparation, occurring only when the normally present GTP of intact rods has been lost.

To separate the kinetics of the first equilibrium reaction, MI ⇌ MII, from the subsequent slower stabilization with Γ, we either discarded the results of the first flash or prepared the RDM under red light. In either case, about 10% of the rhodopsin was bleached, and subsequent bleaches resulted in little or no enhanced MII formation; that is, the logarithmic decrement plots were essentially linear from the first flash.

To improve the signal to noise ratio, data from each flash were averaged, and the composite was fit to a single exponential by using a least-squares method. The exponent of this best-fit curve is k_{obs}. The forward rate constant k_1 was determined from the slope of this curve, extrapolated back to the time of the flash, and divided by Δe[Rh] (eq 11). To correct for the difference between the initial rhodopsin concentration and the average concentration in the composite, the logarithmic decrement curve was used to determine the ratio between the ΔOD of the first bleach (or what would have been the ΔOD if there had been no MII enhancement) and the ΔOD of the composite (Figure 1).

The kinetic theory was developed in terms of the absorbance of the RDM suspension, yet what is measured is the optical density, so that the effects of scattering on the measurements must be considered. Since all measurements are in terms of changes in the optical density on bleaching, we need only be concerned with changes in the scattering on bleaching. The greater part of these changes is corrected for by subtracting, as a reference signal, the change in optical density at 650 nm. Further, any change in scattering which is rapid relative to the formation of MII (e.g., concomitant with loss of rhodopsin, formation of MI, etc.) is excluded from subsequent analysis, since the ΔOD is only measured from the top of this initial pedestal. The goodness of fit of the data to a single exponential argues that any slower scattering change either is negligibly small or has a time constant close to, if not identical with, that of the formation of MII. Finally, the linearity of the logarithmic decrement curve shows that this component of the scattering, if significant, is proportional to the MII formed. But the Δe of the MI → MII transition was determined from just such measurements. Thus, to the extent that there is a scattering change concurrent with and proportional to the formation of MII, the numerical value of Δe would reflect the difference in (molar) optical density rather than in molar absorbance.

Results

A typical set of data is shown in Figure 2. This shows the results of five experiments done at 5.5 °C with aliquots of the same preparation adjusted to different values of pH. Several points may be noted: (1) The amplitude of the change in optical density increases as the pH is lowered, because the higher proton concentration shifts the equilibrium toward MII. (2) The initial slope increases with lower pH, since the rate of formation of MII is accelerated by increasing proton concentration (mass action). (3) The time required for the reaction to reach equilibrium increases as the pH is lowered to

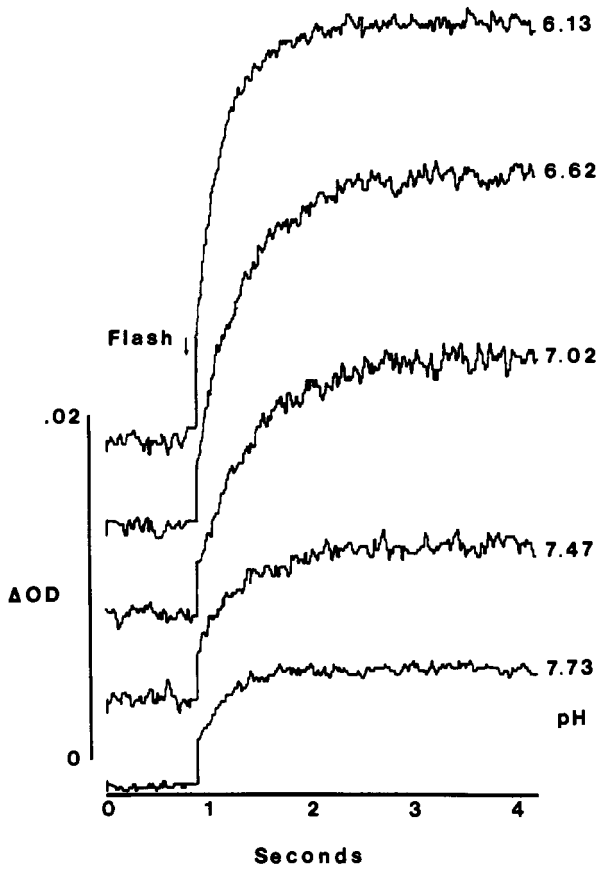

FIGURE 2: Typical results from one set of experiments. A set of kinetic response curves are shown for the MI ⇌ MII equilibrium at 5.5 °C and five different pHs. Note that as the pH decreases, the response becomes larger since more MII is formed, the initial slope increases since k_1 is increasing, and the time to equilibrium becomes first longer and then shorter since k_{obs} has a minimum near pH 7 at this temperature.

a point near neutrality and then decreases as the preparation is further acidified. Thus, the observed rate constant of the reaction (k_{obs}) has a minimum near pH 7 at 5 °C. At higher temperatures, the results appear similar, except that the reaction goes to completion more rapidly.

Over 100 such experiments were done, including 27 pairs of duplicates, at temperatures between −1 and 15 °C and between pH 5.9 and 8.1, and the rate constants k_{obs}, k_1, and k_{-1} were determined for each experiment. For reduction of these data to a single set of equations, two independent theoretical relationships were needed for the rate constants as a function of temperature and pH. The first one was provided by the van't Hoff equation in the following way:

The equilibrium constant for the reaction MI + nH$^+$ ⇌ MII is defined as

$$K_{eq} = [\text{MII}]/([\text{MI}][\text{H}^+]^n)$$

where n is as defined in eq 1. K_{eq} is related to the temperature and, implicitly, the pH of the reaction by the van't Hoff equation:

$$\mathrm{d}(\ln K_{eq})/\mathrm{d}T = \Delta H^\circ/(RT)$$

If ΔH° is constant over temperature, this can be integrated to

$$\ln K_{eq} = -\Delta H^\circ/(RT) + \Delta S^\circ/R$$

In most proteins that have been studied, the pH dependence of ΔH is nearly equal to that of ΔS and of opposite sign [See, for example, Johnson et al. (1963)]. Thus, there is little net

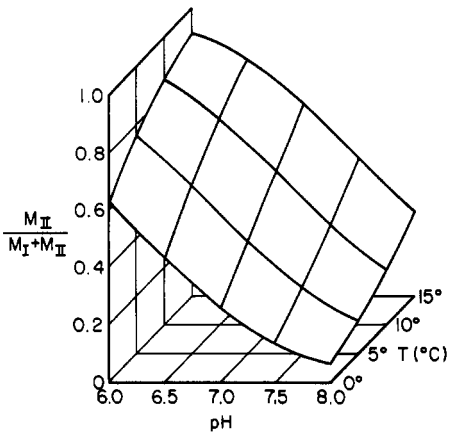

FIGURE 3: Surface plotting [MII]/([MI] + [MII]) as a function of pH and temperature. This is derived from eq 13b: ln ([MI]/[MII]) = −9464(1/T) − 1.608pH + 44.87. Rulings are at pH 6.0, 6.5, 7.0, 7.5, and 8.0 and at 0, 5, 10, and 15 °C.

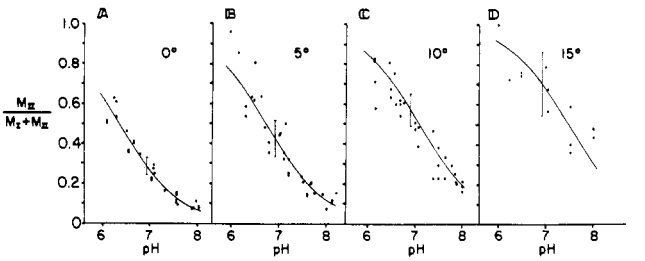

FIGURE 4: Data points for the function [MII]/([MI] + [MII]). These have been projected onto the nearest constant-temperature plane, either 0 (A), 5 (B), 10 (C), or 15 °C (D), correcting for differences between nominal and actual temperatures. Constant-temperature curves are as shown in Figure 3. Error bars show standard errors for each set of data.

pH dependence from these terms. If this is true for rhodopsin, the pH dependence in the equilibrium constant can be explicitly displayed, and the equation becomes

$$\ln([\text{MII}]/[\text{MI}]) = \ln(k_1/k_{-1}) = -\Delta H^\circ/(RT) - 2.303n(\text{pH}) + \Delta S^\circ/R \quad (13a)$$

Since [MII]/[MI], T, and pH were known for each experiment, it was possible to fit all of our data to a two-way linear regression[3] of ln ([MII]/[MI]) on 1/T and pH. This was done for 103 experiments, giving the result (standard errors are shown in parentheses)

$$\ln([\text{MII}]/[\text{MI}]) = -9464(\pm 968)(1/T) - 1.608(\pm 0.097)\text{pH} + 44.87 \quad (13b)$$

From these results, the nonplanar surface that plots [MII]/([MI] + [MII]) as a function of T and pH was derived. This surface is shown in Figure 3, with rulings at 0, 5, 10, and 15 °C and at pH 6.0, 6.5, 7.0, 7.5, and 8.0. The surface is nearly planar except in the region around pH 8 and 0 °C, where it turns up, and in the opposite corner near pH 6 and 15 °C, where it turns down.

A measure of the goodness of fit can be seen in Figure 4A–D, where the data points are projected onto the nearest constant-temperature planes by using the temperature coefficient in eq 13b to correct for the difference between the nominal and actual temperatures. On each graph, the standard error in estimating [MII]/([MI] + [MII]) from pH and

[3] Calculations were done with the 1981 BMDP Statistical Software program, Department of Biomathematics, University of California, Los Angeles, CA.

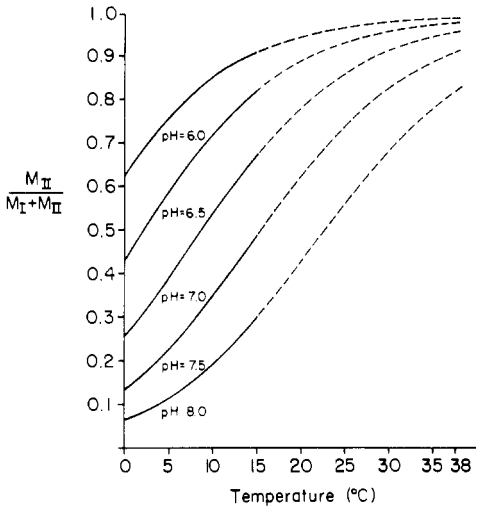

FIGURE 5: Temperature dependence of [MII]/([MI] + [MII]). These curves plot [MII]/([MI] + [MII]) as a function of temperature for different values of pH by using eq 13b. The dashed lines extrapolate from the data to 38 °C.

temperature for the points included in that graph is plotted. The random error is strongly temperature dependent, increasing with increasing temperature for the reasons discussed above. Figure 5 plots the temperature dependence of [MII]/([MI] + [MII]), extrapolated to 38 °C, for different values of pH.

Equation 13 provides estimates for $\Delta H°$ and n that are derived from all the data, and from these, K_{eq} and the other thermodynamic parameters[4] are calculated. These are

$$n = +0.70 \pm 0.04$$

$$K_{eq} = 27\,000/\text{mol at } T = 0\ °C$$

$$\Delta H° = +18\,800 \pm 1900 \text{ cal/mol}$$

$$\Delta G° = -5530 \text{ cal/mol at } T = 0\ °C$$

$$\Delta S° = +89.1 \pm 7.0 \text{ eu}$$

Since [MII]/[MI] = k_1/k_{-1}, eq 13a provides one function of the rate constants. To obtain the best-fit values for the individual rate constants, a second, linearly independent equation is needed. This is provided by combining the theories of absolute reaction rates and of acid–base catalysis. The former states that the rate at which a reaction proceeds is proportional to the concentration of activated intermediate so that the temperature dependence of the rate constant leading to this intermediate is given by

$$\ln k = -E_a/(RT) + \text{constant}$$

where E_a is the activation energy of the intermediate [see, for example, Mahler & Cordes (1963)]. The pH dependence of the reaction rate can in turn be obtained from the theory of acid–base catalysis, which gives

$$\ln k = -2.303n^*(\text{pH}) + \text{constant}$$

(For a base-catalyzed reaction, n^* would normally be negative.) Combining these, we can write

$$\ln k = -E_a/(RT) - 2.303n^*(\text{pH}) + \text{constant} \quad (14a)$$

Since k_1 was directly measured (whereas k_{-1} was calculated from k_1 and k_{obs}), a second two-way linear regression was performed for $\ln k_1$ on $1/T$ and pH for all the data points, giving

$$\ln k_1 = -21028(\pm 589)(1/T) - 0.702(\pm 0.059)\text{pH} + 80.01 \quad (14b)$$

From this equation, the surface plotting k_1 as a function of T and pH was calculated, and is shown in Figure 6.

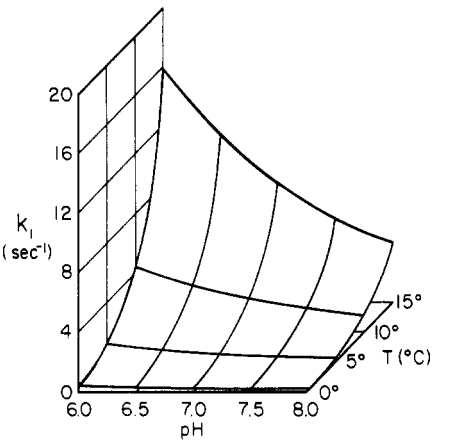

FIGURE 6: Surface plotting k_1 as a function of pH and temperature. The function is derived from eq 14b: $\ln k_1 = -21028(1/T) - 0.702\text{pH} + 80.01$. Rulings are as in Figure 3.

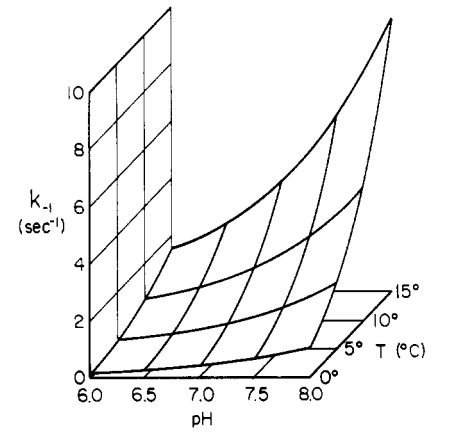

FIGURE 7: Surface plotting k_{-1} as a function of pH and temperature. The function is derived from eq 15: $\ln k_{-1} = -11564(1/T) + 0.906\text{pH} + 35.14$. Rulings are as in Figure 3.

Equations 14a and 14b give the thermodynamic parameters[5] for the activated intermediate M*:

$$E_a = +41\,800 \pm 1200 \text{ cal/mol}$$

$$n^* = +0.30 \pm 0.025$$

$$K^* = 2.55 \times 10^{-14}$$

$$\Delta H^* = +41\,200 \pm 1200 \text{ cal/mol}$$

$$\Delta G^* = +16\,970 \text{ cal/mol at } T = 0\ °C$$

$$\Delta S^* = +88.8 \pm 2.5 \text{ eu}$$

From eq 13b and 14b, the equation of the plane describing $\ln k_{-1}$ can be obtained by subtraction:

$$\ln k_{-1} = -11564(1/T) + 0.906\text{pH} + 35.14 \quad (15)$$

[4] $K_{eq} = k_1 10^{n(\text{pH})}/k_{-1}$, $\Delta G° = -RT \ln K_{eq}$ [$R = 1.987$ cal/(mol·deg)], and $\Delta S° = (\Delta H° - \Delta G°)/T$.

[5] $K^* \equiv [M^*]/[MI] = k_1 h/(\kappa kT)$ ($h = 6.62 \times 10^{-27}$ erg-s, $k = 1.38 \times 10^{-16}$ erg/deg, and $\kappa \simeq 1$), $\Delta H^* = E_a - RT$, $\Delta G^* = -RT \ln K^*$, and $\Delta S^* = (\Delta H^* - \Delta G^*)/T$.

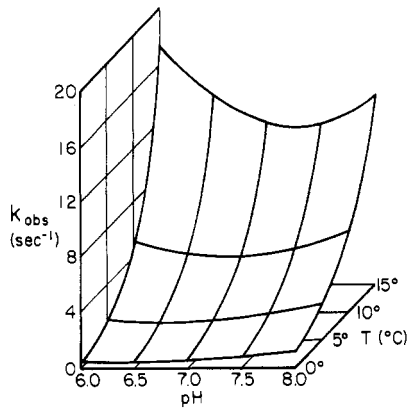

FIGURE 8: Surface plotting k_{obs} as a function of pH and temperature. The function is derived from those for k_1 and k_{-1}. Rulings are as in Figure 3.

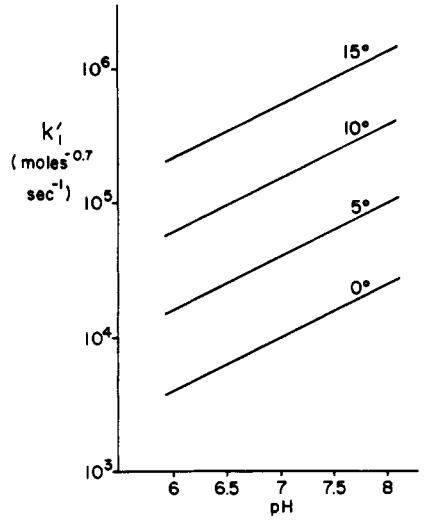

FIGURE 9: True forward rate constant, k'_1, plotted as a function of pH for four temperatures. The Q_{10} of the rate constant is about 15 at 0 °C, decreasing slightly with increasing temperature.

The surface representing k_{-1} as a function of T and pH is shown in Figure 7. Finally, the best-fit surface calculated for $k_{obs} = k_1 + k_{-1}$ is shown in Figure 8, and the values for $k'_1 = k_1/[H]^{0.7}$ are shown in Figure 9. It is noted that k'_1 has a Q_{10} of about 15, the value decreasing slightly with increasing temperature.

The effects of aging on the kinetics of RDM suspensions were investigated at three pHs: 7.95, 7.20, and 6.45. Aliquots from each were analyzed on the day they were prepared, and for 6 days thereafter. The value of k_{obs} for each of the samples declined about 3% per day. The rate constants k_1 and k_{-1} individually declined at about the same rate as k_{obs}, although in all three cases k_1 decreased slightly less than k_{-1}, so that with age the equilibrium shifted slightly toward MII.

Discussion

MI and MII are known to exist, under conditions near room temperature and pH 7, in a rapid equilibrium containing significant fractions of each species. The reversibility of this equilibrium is readily demonstrated, as in our experiments. It has been long recognized that the equilibrium is sensitive to temperature and pH (Matthews et al., 1963), and it has more recently been found to be affected by pressure (Lamola et al., 1974; Attwood & Gutfreund, 1980). The back-reaction is sufficiently rapid that the equilibrium is essentially undisturbed by the slower reactions which proceed from MII: formation of metarhodopsin III or separation into opsin and free retinal.

Kinetic analysis of the approach to equilibrium following flash bleaching of rhodopsin, as determined by monitoring absorbance changes, has produced several different results. Some investigators have found the kinetics to be accurately described as a single first-order process, as would be predicted from the reaction scheme MI $\rightleftharpoons$ MII (Applebury et al., 1974; Rapp, 1979; von Sengbusch & Stieve, 1971). Others have found that two or more exponentials are required to adequately describe the process (Williams, 1970; Abrahamson & Wiesenfeld, 1972; Stewart et al., 1976; Hoffman et al., 1978), and a number of explanations have been offered to explain why the reaction is more complex than originally proposed by Matthews et al. (1963). It has been suggested that there are two different forms of rhodopsin, each with its own kinetic parameters (Williams, 1970). The equilibrium kinetics depend on the nature and amount of associated lipid (Shichi et al., 1977), suggesting that some of the rhodopsin may be partially denatured in the preparative procedure by an alteration of the lipid composition. Changes in light scattering induced by bleaching also affect the apparent kinetics (Uhl et al., 1978; Kuhn et al., 1981).

A probable explanation for at least some of the apparent biphasic response in RDM preparations lies in the stabilization of MII upon binding to Γ, since the latter reaction proceeds more slowly than the initial formation of the MI–MII equilibrium (Emeis & Hofmann, 1981). This would also explain why measurements done on intact retinas generally give a monophasic response (Hagins, 1956; Cone & Cobb, 1969), since in the intact retina endogenous GTP immediately releases the MII from the Γ·GTP complex, preventing any enhanced MII formation. Our results were generally well fit by a single first-order exponential, when those records showing enhanced MII formation were eliminated, as noted above.

The MI–MII equilibrium has been said to be both acid and base catalyzed, on the basis of the U-shaped appearance of k_{obs} when plotted against pH (Emrich & Reich, 1974). With the individual rate constants separately identified, the true forward and backward rate constants are seen to be base catalyzed only. The increase in the pseudo-first-order forward rate constant in more acid pH is due to the mass-action effect of the proton taken up in the conversion to MII. The base catalysis appears to be specific rather than general, since changing the concentration of buffer or rhodopsin or switching to a phosphate buffer does not significantly alter the measured rate constants. However, if the forward reaction is base catalyzed, why is n^* positive? The probable explanation is that the proton is also taken up during the transition from MI to M^*.

Since $\Delta S°$ and ΔS^* are virtually identical, it appears that the conformational change occurring between MI and MII all takes place between MI and M^*. Schematically, the reaction would seem to proceed as shown in Figure 10. That the reaction proceeds as rapidly as it does with such a large enthalpy of activation is due to the large positive entropy associated with the transition. From the amino acid sequence of rhodopsin, the molecule appears to contain seven hydrophobic regions, each of which spans the rod disk membrane (Hargrave et al., 1983). There is evidence from circular dichroism studies on rhodopsin (Shichi, 1971) that bleaching produces no change in the α-helix content of the protein. Thus, the conformational change would seem to involve a reorientation of the helices within the membrane. Since pressure studies have shown that MII is "larger" than MI (Lamola et

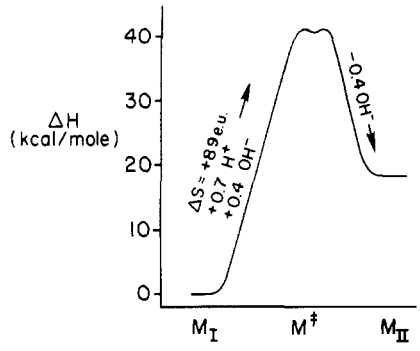

FIGURE 10: Schematic illustrating the thermodynamic parameters for the transition MI → M* → MII. The figures for proton and hydroxyl ion movement assume that all the proton uptake occurs in the transition from MI to M*.

al., 1974; Attwood & Gutfreund, 1980), the reorientation might involve a splaying of the previously parallel-oriented helices in response to the introduction of the charged group, with a consequent greater degree of randomness indicated by the large increase in entropy. The decrease in intrinsic birefringence, with kinetics identical with those of MII formation (Liebman et al., 1974), is consistent with this interpretation, as is the loss in amide II band dichroism seen upon bleaching (Michel-Villaz et al., 1979).

Using the temperature dependence of the data, it is possible to make an estimate of the reaction parameters in the physiologic temperature region near 38 °C. Figure 5 predicts that at 38 °C and pH 7.6, over 90% of the bleached rhodopsin is in the form of MII. If MII can catalyze the binding of GTP to Γ while MI cannot, then the more MII formed, the faster and more efficient will be the activation of Γ and PDE, and the greater the gain of the system; that is, more cGMP's will be hydrolyzed per photon absorbed. Thus, the predicted shift in the MI–MII equilibrium should increase both the speed and sensitivity of the response. Such an effect has recently been demonstrated (Parkes & Liebman, 1982).

Perhaps the most perplexing aspect of the equilibrium between MI and MII concerns the proton taken up in the reaction. Protonation should be rapid relative to the conformational change that accompanies the transition from MI to MII, raising the question as to which comes first. If the protonation occurs in a single step, the most general reaction would be

$$\begin{array}{ccc} MI + nH^+ & \rightleftharpoons & MI \cdot nH^+ \\ \Downarrow\Uparrow & & \Downarrow\Uparrow \\ MII + nH^+ & \rightleftharpoons & MII \cdot nH^+ \end{array}$$

The protonation may precede the conformational change, rendering the latter more likely, or it may follow the conformational change and function to stabilize it. The data presented here do not help to resolve this question, since the transition from MI to M* appears to involve both the conformational change and the proton uptake.

A second question concerns the number of protons taken up in the transition from MI to MII. Here one must distinguish between an essential proton, without which the conversion will not take place, and a nonessential proton, which, due to exposure to the external medium or changing pK of a protonatable site, may be acquired in consequence of the conversion to MII if the medium is sufficiently acid, but whose absence will not affect the conversion. Clearly, some protonation is essential or it would not be possible to alter the equilibrium by changing the pH of the medium, and experiments which, by their design, measure the number of essential protons suggest that about one proton per rhodopsin is required (Wong & Ostroy, 1973). It seems equally clear from other data that there are some nonessential protons taken up as well, as such measurements may yield values of two or more total protons taken up (Bennett, 1978; McConnell et al., 1968).

What meaning can be ascribed to an apparently fractional value (0.7) for an essential proton? This lack of convergence between the effect of pH on the MI–MII equilibrium and the titration curve of a monoprotic indicator base was first noted by Matthews et al. (1963). Although they did not report a value for n, analysis of their data (Figure 3, op. cit.) yields a figure of about 0.60. They believed that the discrepancy might be due to the ionic strength of their solvent (0.17 M phosphate buffer). Abrahamson & Wiesenfeld (1972) observed a pH dependence of the equilibrium approximately equal to the square root of the hydrogen ion concentration and suggested that the value of n might be uninterpretable in a reaction which they believed proceeded with three different time constants. Other authors, while not specifically commenting on the discrepancy, have reported titration data that clearly show an effective value for n of less than 1 (Radding & Wald, 1956; McConnell et al., 1968).

The agreement among so many investigators suggests that the apparent fractional value for n is not just due to a systematic experimental error. But whether the actual value of n is less than 1 depends on the validity of our earlier assumption that rhodopsin has little net pH dependence in its enthalpy and entropy. A net pH dependence of 1.38 kcal mol^{-1} (pH unit)$^{-1}$ would give n a value of 1. (This is not a large pH dependence for either ΔH or ΔS, but it is a very large net dependence.) If, on the other hand, the fractional value of n is real, it rules out the simplest hypothesis, that is, that a specific site is always protonated for MII and never for MI. The exponent would then represent a time or statistical average of some underlying stochastic process.

Conclusion

We have developed two equations (13b and 14b) which appear to give reasonably accurate estimates of K_{eq}, k_1, k_{-1}, and k_{obs} for the MI–MII equilibrium within the range of 0–15 °C and pH 6–8. A faster flash photometer should permit us to extend the effective range of these equations to higher temperatures. Although a question remains as to the interpretation of the values obtained for n and n^*, this does not affect the usefulness of these equations for estimating equilibrium and rate constants, and the thermodynamic parameters.

Acknowledgments

We thank Dr. S. Walter Englander and Dr. Roland G. Kallen for helpful discussions.

Registry No. Hydrogen ion, 12408-02-5.

References

Abrahamson, E. W., & Wiesenfeld, J. R. (1972) in *Handbook of Sensory Physiology* (Dartnall, H. A. J., Ed.) Vol. VII, Part 1, pp 69–121, Springer-Verlag, West Berlin.

Applebury, M. L., Zuckerman, D. M., Lamola, A. A., & Jovin, T. M. (1974) *Biochemistry 13*, 3448–3458.

Attwood, P. V., & Gutfreund, H. (1980) *FEBS Lett. 119*, 323–326.

Baumann, Ch. (1978) *J. Physiol. (London) 279*, 71–80.

Baumann, Ch., & Reinheimer, R. (1973) in *Biochemistry and Physiology of Visual Pigments* (Langer, H., Ed.) pp 89–99,

Springer-Verlag, West Berlin.
Baumann, Ch., & Zeppenfeld, W. (1981) *J. Physiol. (London) 317*, 347–364.
Bennett, N. (1978) *Biochem. Biophys. Res. Commun. 83*, 457–465.
Bennett, N., Michel-Villaz, M., & Kühn, H. (1982) *Eur. J. Biochem. 127*, 97–103.
Cone, R. A., & Cobb, W. H., III (1969) *Nature (London) 221*, 820–822.
Ebrey, T. G. (1968) *Vision Res. 8*, 965–982.
Emeis, D., & Hofmann, K. P. (1981) *FEBS Lett. 136*, 201–207.
Emrich, H. M., & Reich, R. (1974) in *Biochemistry of Sensory Functions* (Jaenicke, L., Ed.) pp 23–27, Springer-Verlag, West Berlin.
Falk, G., & Fatt, P. (1966) *J. Physiol. (London) 183*, 211–224.
Hagins, W. A. (1956) *Nature (London) 177*, 989–990.
Hargrave, P. A., McDowell, J. H., Curtis, D. R., Wang, J. K., Juszczak, E., Fong, S. L., Mohana Rao, J. K., & Argos, P. (1983) *Biophys. Struct. Mech. 9*, 235–244.
Hoffmann, W., Siebert, F., Hofmann, K. P., & Kreutz, W. (1978) *Biochim. Biophys. Acta 503*, 450–461.
Johnson, F. H., Eyring, H., & Polissar, M. J. (1963) *The Kinetic Basis of Molecular Biology*, pp 274–275, Wiley, New York.
Knowles, A., & Dartnall, H. J. A. (1977) in *The Eye* (Davson, H., Ed.) Vol. 2B, p 66, Academic Press, New York.
Kühn, H., Bennett, N., Michel-Villaz, M., & Chabre, M. (1981) *Proc. Natl. Acad. Sci. U.S.A. 78*, 6873–6877.
Lamola, A. A., Yamane, T., & Zipp, A. (1974) *Biochemistry 13*, 738–745.
Lewis, J. W., Winterle, J. S., Powers, M. A., Kliger, D. S., & Dratz, E. A. (1981) *Photochem. Photobiol. 34*, 375–384.
Liebman, P. A., & Pugh, E. N., Jr. (1979) *Vision Res. 19*, 375–380.
Liebman, P. A., & Pugh, E. N., Jr. (1981) *Curr. Top. Membr. Transp. 15*, 157–170.
Liebman, P. A., Jaeger, W. S., Kaplan, M. W., & Bargoot, F. G. (1974) *Nature (London) 251*, 31–36.
Liebman, P. A., Mueller, P., & Pugh, E. N., Jr. (1983) *J. Physiol. (London) 347*, 85–110.
Mahler, H. R., & Cordes, E. H. (1966) *Biological Chemistry*, pp 268–271, Harper and Row, New York.
Matthews, R. G., Hubbard, R., Brown, P. K., & Wald, G. (1963) *J. Gen. Physiol. 47*, 215–240.
McConnell, D. G., Rafferty, C. N., & Dilley, R. A. (1968) *J. Biol. Chem. 243*, 5820–5826.
Michel-Villaz, M., Saibil, H. R., & Chabre, M. (1979) *Proc. Natl. Acad. Sci. U.S.A. 76*, 4405–4408.
Mueller, P., & Pugh, E. N., Jr. (1983) *Proc. Natl. Acad. Sci. U.S.A. 80*, 1892–1896.
Ostroy, S. E., Erhardt, F., & Abrahamson, E. W. (1966) *Biochim. Biophys. Acta 112*, 265–277.
Parkes, J. H., & Liebman, P. A. (1982) *Invest. Ophthalmol. Visual Sci. Suppl. (ARVO) 22*, 44.
Parkes, J. H., Liebman, P. A., & Pugh, E. N., Jr. (1979) *Invest. Ophthalmol. Visual Sci. Suppl. (ARVO) 18*, 22.
Radding, C. M., & Wald, G. (1956) *J. Gen. Physiol. 39*, 909–922.
Rafferty, C. (1979) *Photochem. Photobiol. 29*, 109–120.
Rapp, J. (1979) *Vision Res. 19*, 137–141.
Shichi, H. (1971) *J. Biol. Chem. 246*, 6178–6182.
Shichi, H., Muellenberg, C. G., Hărosi, F. I., & Somers, R. L. (1977) *Vision Res. 17*, 633–636.
Somers, R. L., & Shichi, H. (1982) *Invest. Ophthalmol. Visual Sci. Suppl. (ARVO) 22*, 43.
Stewart, J. G., Baker, B. N., Plante, E. O., & Williams, T. P. (1976) *Arch. Biochem. Biophys. 172*, 246–251.
Uhl, R., Hofmann, K. P., & Kreutz, W. (1978) *Biochemistry 17*, 5347–5352.
von Sengbusch, G., & Stieve, H. (1971) *Z. Naturforsch., 26B*, 861–862.
Williams, T. P. (1970) *Vision Res. 8*, 525–533.
Wong, J. K., & Ostroy, S. E. (1973) *Arch. Biochem. Biophys. 154*, 1–7.
Yee, R., & Liebman, P. A. (1978) *J. Biol. Chem. 253*, 8902–8909.